The MicroBooNE Search for Single Photon Events Public Note 1041

The MicroBooNE Collaboration

July 7, 2018

Abstract

This note describes and presents preliminary results for the MicroBooNE analysis being developed to search for neutrino-induced neutral current single photon events in the MicroBooNE detector. The analysis currently assumes neutrino neutral current Δ production followed by Δ radiative decay on argon (NC $\Delta \to N\gamma$) as the "signal model"; event reconstruction and selection have been developed and are being optimized in order to reduce cosmogenic and other beam-related backgrounds explicit to the NC $\Delta \to N\gamma$ process. This note presents the current status of event reconstruction, selection, optimization and validation checks for the early stages of analysis on external (cosmogenic background) events. Also presented are the projected sensitivities for testing the standard model predicted rate for the NC $\Delta \to N\gamma$ process and for testing the interpretation of the previously observed MiniBooNE low energy excess as NC $\Delta \to N\gamma$ events.

1 Introduction

The MicroBooNE detector [1] is a 170 ton (85 ton active mass) liquid argon time projection chamber (LArTPC) located on the Booster Neutrino Beamline (BNB) at Fermilab. Its primary physics goals include a suite of measurements of neutrino-argon interaction cross-sections at the ∼0.1-1.5 GeV neutrino energy range, and the investigation of the "low energy excess" (LEE) of events observed in the MiniBooNE experiment [2], which shares the same beamline as MicroBooNE. To this date, this excess observation remains both unexplained and unconfirmed. Its interpretations vary and can generally be divided into "electron-like" and "photon-like" interpretations, due to MiniBooNE's inability to differentiate between electron and photon electromagnetic showers. The analysis described in the following sections partly addresses the latter interpretation.

This note describes and provides preliminary validation results from an ongoing MicroBooNE physics analysis effort to isolate a sample of BNB neutrino interactions in the MicroBooNE detector that are characterized by *a single photon and no lepton* in the final state, consistent with the "photon-like" interpretation of the MiniBooNE LEE. This interaction topology is consistent with that of neutrino neutral current (NC) Δ baryon production, followed by Δ radiative decay, $\Delta \to N\gamma$, where $N = p, n$; therefore, for definitiveness, the analysis assumes this specific channel as its sample of interest (the *signal* sample). The analysis could be readily extended and further optimized for studying other "single photon and no lepton" processes in MicroBooNE in the near future.

Other processes which are consistent with the MiniBooNE "single photon and no lepton" LEE interpretation involve the following NC processes: mis-estimated backgrounds (most dominantly contributed by mis-identified NC π^0 events in MiniBooNE), or unaccounted-for neutrino NC interaction processes. These could be the result of NC-like new physics or standard model predicted processes which may have been mis-estimated or mis-modeled; an example of the latter is anomaly mediated single photon production in neutrino scattering [3] (a standard model predicted process, but which currently stands unmeasured and has

a large cross-section uncertainty associated with it).

The search presented in this note focuses exclusively on the NC $\Delta \to N\gamma$ channel, which for BNB neutrino energies involves predominantly the $\Delta(1232)$[1]. Due to their extremely short lifetime, all produced Δ's decay in the nucleus where they are produced and are reconstructable only from their decay final state topologies. The largest decay branching ratio of Δ decay is that of $\Delta \to N\pi$, at 99.4%, with the remaining branching fraction being that of decay into a single photon plus a lighter nucleon N (proton or neutron), $\Delta \to N\gamma$. Although the radiative Δ decay has been observed in electron scattering experiments, it has never been directly measured with Δ's produced in neutrino scattering.

The exact rate of radiative Δ decay is not fixed by the branching ratio alone. As the Δ is produced on resonance, the overall rate of this process is also proportional to the neutrino NC resonant cross-section for argon. In addition, the lower energy Δ cannot produce an on shell π^0 and so this decay mode is suppressed at lower energy exchange. For the analysis presented in this note, the default cross-section and radiative decay branching fraction available in the GENIE neutrino event generator v02_12_02 [4] are used. This low-energy dependence is included in the GENIE modeling of the resonance.

2 Single Photon Search Analysis Description

2.1 Analysis Outline

NC Δ radiative decays produce a variety of topologies in a LArTPC detector. In this analysis there are two distinct topological selections that are carried out independently of each other:

- $1\gamma 0p$**:** The most common topology corresponds primarily to NC Δ^0 production followed by $\Delta^0 \to n\gamma$, in which a sole shower is the only reconstructible object. This is a difficult topology, but is worth studying due to the low statistics of the signal in general. This topology accounts for 40% of the vertices in our signal sample.

- $1\gamma 1p$**:** The inclusion of a proton track allows for significant improvements to cosmogenic background rejection, as the track directionality and calorimetry of beam-related protons are quite distinct from cosmic muons and cosmic muon induced backgrounds in the MicroBooNE detector. In addition, having a track associated to a shower gives a better-defined vertex position, which allows one to study the photon conversion distance in order to further reject electron shower backgrounds from intrinsic ν_e charged-current interactions. This topology accounts for 55% of vertices in our signal sample.

The analysis explicitly targets candidate neutrino interaction topologies with one (1) photon-like shower, and zero (0) or one (1) proton-like tracks associated with the reconstructed neutrino interaction vertex. The analysis can be performed exclusively on either 0-track ($1\gamma 0p$) or 1-track ($1\gamma 1p$) topologies, or on an inclusive combination of the two samples (which are otherwise mutually exclusive). At present the statistical-only sensitivity to NC Delta radiative event signals is slightly higher for the combined case, as shown at the end of this note. Due to final state interactions, one cannot make the direct connection between an observed topology and the underlying decay, e.g $1\gamma 1p$ cannot be assumed to be due to $\Delta^+ \to p\gamma$ as the observed proton could have been knocked out of the nucleus by the neutron in a $\Delta^0 \to n\gamma$ decay. Thus although motivated by their respective Δ decays, the $1\gamma 0p$ and $1\gamma 1p$ selections should be thought of as topological selections only.

The analysis builds on MicroBooNE Monte Carlo (MC) and data which have been reconstructed using the Pandora framework [5]. We begin with Pandora reconstructed tracks and showers, after cosmic ray activity removal[2], that are reconstructed as part of Pandora candidate neutrino interaction vertices. Rather

[1] Heavier excitations at 1,400 MeV, 1,520 MeV and 1,535 MeV are produced markedly less at the BNB neutrino energy range, accounting for less than 5% of the total single-photon cross-section.

[2] This stage is necessary as MicroBooNE is situated on surface and is subject to large cosmogenic backgrounds.

than utilizing the Pandora vertices, the tracks and showers in any given LArTPC drift readout (simulation or data) are subsequently run through a neutrino interaction vertex reconstruction algorithm, described in Sec. 2.2. This "VertexBuilder" is specifically designed for the single-photon topology of interest in mind, and is furthermore explicitly optimized (using Monte Carlo simulation) for maximal reconstruction efficiency of true NC Δ radiative signal events.

The analysis selection begins with any reconstructed neutrino interaction candidate vertex per given drift readout (recorded "event") that has only a single reconstructed shower associated with it. Multiple candidate vertices are allowed per event, though ultimately we expect only one vertex per event to survive final selection. The selected candidate vertices are subsequently run through various analysis selection stages. In particular, reconstructed neutrino interaction candidate vertices with only one (1) shower associated with the vertex are pre-selected according to their timing (in coincidence with the BNB beam spill window) and other low-level information to help isolate (truly) beam-related neutrino signals, and reject beam-unrelated activity, as described in Sec. 2.3. The pre-selected candidate vertices for each of the two separate samples ($1\gamma 0p$ and $1\gamma 1p$) are then separately run through a series of two boosted decision trees (BDT's) designed and trained explicitly for the reduction of cosmogenic single-shower backgrounds and other beam-related single-shower backgrounds. The two BDT's are described in detail in Sec. 2.4. The resulting reconstruction and selection efficiencies and corresponding Monte Carlo predicted distribution of events for the MicroBooNE data set corresponding to 6.6E20 protons on target (POT) are provided in Sec. 2.5. Background investigations are presented in Sec. 2.6

In order to validate the analysis, Monte Carlo predictions are compared to data as a function of reconstructed shower energy for the early selection stages, using the currently unblinded MicroBooNE data set corresponding to 5E19 POT in Sec. 3. This data sample is expected to have negligible signal contribution. The Monte Carlo prediction for the final spectra consists of the LEE Δ radiative signal, stacked on top of both the BNB Monte Carlo backgrounds as well as a sample of cosmics coincidence with the beam spill period (in-time cosmics), which is estimated using *in-situ* measurements of cosmics at MicroBooNE via an external (non BNB beam-spill) trigger.

Finally, using the predicted Monte Carlo spectra, including template signal predictions corresponding to the NC Delta single photon interpretation of the MiniBooNE LEE, a statistical-only χ^2 fit is performed in order to quantify MicroBooNE's sensitivity to that hypothesis. The LEE signal prediction in the sensitivity calculations presented in this analysis amounts to roughly a three-fold increase in the normalization of the standard-model-predicted NC Delta radiative decay cross section [6]. This is presented in Sec. 4.

2.2 Vertex Reconstruction

The VertexBuilder takes reconstructed shower and track objects (reco-objects) from an event as input and attempts to associate them with each other. The VertexBuilder has three main input parameters:

- t_{max}: maximum distance at which two tracks can be associated
- b_{max}: maximum distance the shower is backwards-projected
- s_{max}: maximum shower impact parameter for a shower to be associated with another reco-object

When associating tracks the VertexBuilder uses the position of the start and end of the track. The closest two track start/end points in the event within t_{max} of each other will be associated together and a candidate vertex will be created at the midway point between them. Any other tracks within t_{max} of this vertex will also be associated. This process is repeated until there are no more unassociated tracks with start/end points less than t_{max} from each other. Showers in the event are associated with other reco-objects by backwards-projecting the showers (pointing a line in the direction opposite to the shower) a distance b_{max} and finding

the impact parameters between the backwards-projection and each other reco-object. The shower will be associated with the reco-object it makes the smallest impact parameter with, if that impact parameter is less than s_{max}. Currently Pandora is used to the produce the reco-objects used as input by the VertexBuilder. Once track and shower association has been performed the VertexBuilder will output a selection of vertices with *at least* one associated shower and any number of associated tracks. There can be (and often are) multiple candidate vertices per event at this stage.

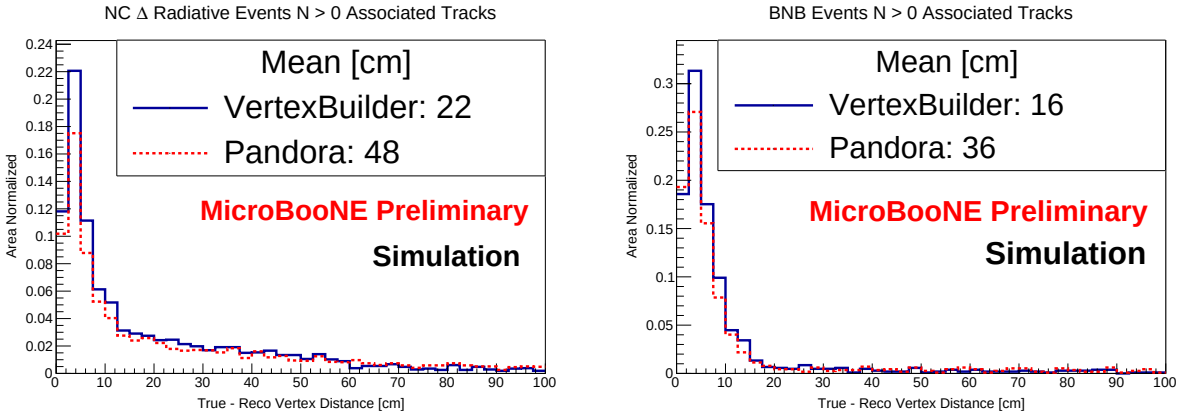

Figure 1: *Plots showing the 3-d distance between reconstructed vertices (with at least one associated shower) and true neutrino vertices. The left plot is for MC NC Δ radiative + cosmic events and the right is for MC BNB + cosmic events (area normalized). The reconstructed vertex is required to have at least one track so it has a definite position (lone photon showers convert ∼ 14 cm from the vertex). Distributions shown for the VertexBuilder and default Pandora vertexing. Note that the 3-d distance can be greater than the 100 cm limit on the plot (this is why the two distributions appear to have different integrals).*

Figure 1 shows the vertex resolution of both the VertexBuilder developed for this analysis and default Pandora vertexing for MC NC Δ radiative events overlaid with MC cosmic activity (left) and all other types of MC BNB events overlaid with MC cosmic activity (right). The distributions are area-normalized (the two different vertexing methods return a different number of vertices per event; hence the plots are a shape-only comparison). In both cases we can see that the VertexBuilder performs better in terms of vertex resolution for events with showers. This improved performance arises from the additional backwards projection stage performed by the VertexBuilder allowing photon showers from NC Δ radiative decay and $\pi_0 \rightarrow 2\gamma$ decay (which account for a significant portion of BNB showers) to be correctly associated more frequently. The vertex resolution of the NC Δ radiative sample is worse than the BNB sample due to the larger number of photon showers in the former sample which can be more easily associated with the wrong track than electron showers (∼14 cm photon conversion length).

The vertex reconstruction stage of this analysis returns as a candidate single-photon vertex any reconstructed vertex that has a single shower associated with it, and either zero or one associated tracks. Candidate single-photon vertices are then processed further through subsequent pre-selection and selection stages.

2.3 Pre-selection

After vertex reconstruction, several pre-selection cuts are applied on each candidate single-photon vertex in order to improve first and foremost the quality of the samples that are used for subsequent selection stages, and to a lesser extent the signal to background ratio itself. The following pre-selection cuts are applied to all samples:

- **Fiducial Cut:** Distance from TPC wall to reconstructed vertex < 10 cm in all directions. This cut is used to ensure TPC field uniformity and maximize containment of vertex-related activity.
- **Shower Energy Threshold:** Reconstructed shower energy > 30 MeV. This cut is used to remove showers corresponding to muon decay electrons and to also minimize the presence of "broken showers" which result from imperfect shower reconstruction and would otherwise be considered as candidate primary showers.
- **Track Length Maximum:** Associated track length < 100 cm. This cut is used to remove events with what is likely a muon (long) track, either from cosmic rays or ν_μ charged current (CC) interactions.
- **Distinct photon gap:** Photon conversion distance from reconstructed vertex > 1 cm. This cut is only applicable to the $1\gamma 1p$ sample selection, as in the $1\gamma 0p$ sample the vertex is assumed to be at the shower start position. This cut is used to minimize contributions from ν_e CC events which are characterized by a shower (electron) attached to the vertex, as well as any other background that produces showers in conjunction with a track like object.
- **Sufficient Light in Beam-gate window:** Total number of photoelectrons (PE) inside beam-gate window > 20. This is to minimize beam-unrelated mis-identified events and ensure that the reconstructed vertices are well-reconstructed in time (and therefore in x).
- **"Good" track calorimetry:** A track having at least 5 track hits with sensible dE/dx ($dE/dx < 30$ MeV/cm), and track mean $dE/dx > 1$ MeV/cm over the whole track. [3]
- **Correct Direction of Track:** The ratio of the mean dE/dx over the first half of a track (defined relative to the track start point) to that of the second half (defined relative to the track end point) must be > 1.0. This cut is primarily introduced to remove incorrectly reconstructed tracks that point toward the vertex.
- **Back-to-Back tracks and showers:** The angle between reconstructed track and shower in $1\gamma 1p$ selection must be $\cos\theta_{\gamma p} > -0.95$. This cut is introduced to reduce split track events where one side of the split was reconstructed as a shower.

The individual, and cumulative, effects of these cuts on both the background and signal samples are shown in Tabs. 1 and 2 for the $1\gamma 1p$ and $1\gamma 0p$ topological selections, respectively.

2.4 Background Rejection BDT's

All vertices passing pre-selection cuts are passed into two BDTs trained a priori to reject as many background-like vertices as possible. The variables used in the this selection encompass a variety of geometric, topological, and calorimetric discriminators such as reconstructed shower energy, vertex position, and track length. It is the distributions after the pre-selection cuts have been applied that are used to train the BDTs, allowing them to learn only the well reconstructed features of the signal sample. Two different BDTs are trained for each sample, one primarily to remove cosmic vertices, and a second which focuses on BNB related backgrounds. This staged approach has increased performance over a single combined BDT, due to the fact that the BDT learns more efficiently the characteristics of their focused backgrounds.

[3] For each reconstructed track Pandora calorimetry provides a set of (a) residual range and (b) dE/dx value at each track hit in the track. A track is "good" if the number of hits whose $dE/dx < 30$ MeV/cm is more than 5, after ignoring the first and last point in the track.

2.4.1 Background Rejection BDT Performance

Figure 2 shows the BDT performance for both the cosmic-rejection BDT (top figures) and the BNB background rejection BDT (bottom figures) for the two topologies considered: $1\gamma 1p$ (left figures) and $1\gamma 0p$ (right figures). Each BDT is trained and then tested on statistically independent samples, with cosmic events for training being generated with the corsika cosmic simulation[7]. The BDT response on the test samples is shown on the top panels; the efficiency for both signal and background are shown in the bottom panels. As demonstrated in the figure, in the case of the cosmic-rejection BDT, high (90%) efficiency to signal events is possible for as low as a 1% mis-identification efficiency to cosmic background events, or lower, for both the $1\gamma 1p$ topology and the $1\gamma 0p$. Similarly, for the BNB background-rejection BDT, a high (90%) efficiency to signal events is possible for both $1\gamma 1p$ and $1\gamma 0p$ cases for as low as a $\sim$10% mis-identification efficiency for BNB background events. Further background rejection starts to degrade signal sensitivity. For the signal sample in both BDTs we train on pure signal with no coincidence cosmic contamination.

In the case of the $1\gamma 1p$ sample, much of the power of the cosmic-rejection BDT comes from the fact that cosmic events have very different directionality than beam related neutrino events. This discriminant is shown in the left panel of Fig. 3. The demand that there is a gap between the vertex and reconstructed shower start point of at least 2 cm also greatly helps reduce Michel electron showers from being mis-interpreted as possible photon showers, as demonstrated in the right panel of Fig. 3. In the case of the $1\gamma 0p$ sample, much of the power of the BDT comes from shower directionality as well as the shower dE/dx averaged during the shower's first 4 cm. These discriminants are shown in left and right panels of Fig. 4.

2.5 Final Event Selection

To obtain a final selected sample for each of the topologies under study ($1\gamma 1p$ and $1\gamma 0p$), a cut is placed on each BDT response (cosmic and BNB), which has been determined by independently varying each response cut (cosmic and BNB) and choosing the combination for which a statistical-only significance of $s/\sqrt{b}$ is maximized, where s (b) is the number of selected signal (background) events after the BDT response cuts are applied. The exact values of the cuts chosen to maximize the significance for the $1\gamma 0p$ and the $1\gamma 1p$ topological selections are shown in Tab. 3. Since the two samples are statistically independent, a combination of the two selections can be performed as well, yielding a combined statistical significance of 1.87σ (for 6.6E20 POT).

Although the BDTs were trained on Corsika cosmic Monte Carlo, MicroBooNE has been collecting external cosmic-only data when the BNB neutrino beam is off. This sample represents the most accurate (realistic) sample of cosmogenic backgrounds in MicroBooNE, and it is therefore used in this analysis both as an additional cross-check to ensure that the cosmic rejection BDT behaves similarly for Monte Carlo and data, and as an *in-situ* measured cosmogenic background sample appropriately scaled to represent beam spill coincident cosmic backgrounds in the single photon search.

The primary variable in which we perform the final fits is reconstructed shower energy, as it is common to both studied topologies. In this section, we present how the reconstructed shower energy distribution appears at each stage of the analysis. We normalize all events to 6.6e20 POT and stack the NC Δ radiative LEE signal, BNB backgrounds, and independently *in-situ* measured in beam-spill coincidence cosmic events on top of each other to best estimate the end observable spectrum.

In both topologies, the vertices passed from the VertexBuilder are dominated by cosmic vertices. The pre-selection cuts reduce these by over an order of magnitude, but they remain the dominant background. The pre-selection cuts also introduce quite a large reduction on the signal sample, with a combined efficiency relative of just 34.5%. Nevertheless, even if the pre-selection cuts are relaxed, the BDTs reproduce the cut positions almost exactly, resulting in similar final efficiencies but with generally worse quality events due to

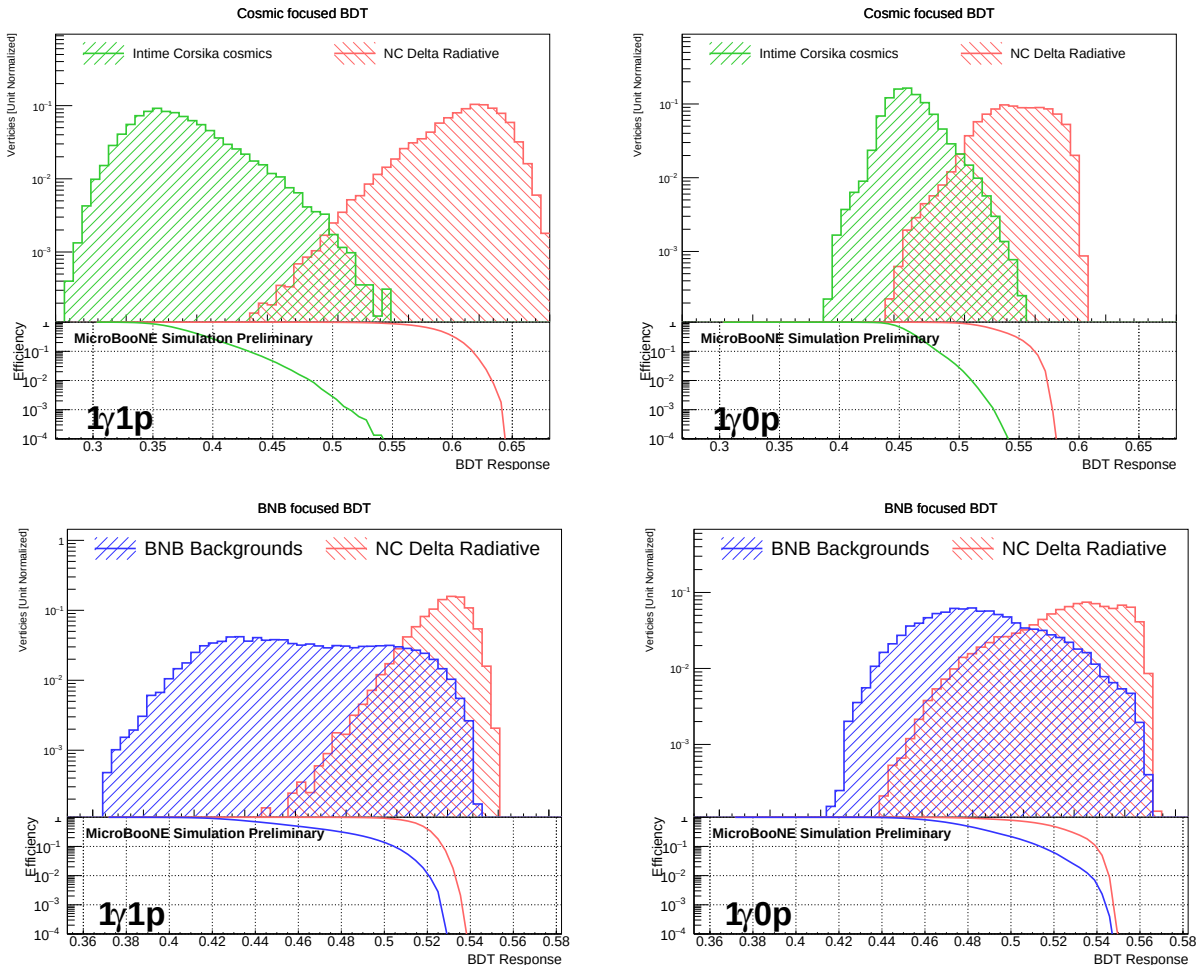

Figure 2: *The BDT performance after training and testing on simulated cosmics ("in-time corsika" shown in green) and the true NC Δ radiative events (shown in red). The top figures correspond to the cosmic-rejection BDT; the bottom figures correspond to the BNB background-rejection BDT. The figures on the left correspond to the $1\gamma1p$ sample; the figures on the right correspond to the $1\gamma0p$ sample. Each figure shows the BDT Response (top panel) and resulting efficiencies for both signal and background (bottom panel). The larger the BDT response, the more signal-like an event is assumed to be. Strong cosmic rejection power can be obtained while retaining large signal efficiencies. Once can see visually that cosmic separation is significantly more powerful than BNB background separation. Similarly, the $1\gamma1p$ topological selection allows for stronger discrimination power that the $1\gamma0p$ selection due to the additional information one has when a track is present.*

training on badly reconstructed vertices.

After applying the BDT trained primarily to reject cosmic vertices, only 26.1 signal events remain in the $1\gamma1p$ selection, whereas 29.6 in the $1\gamma0p$ (scaled to 6.6E20 POT). Although trained on cosmic events, the cosmic BDT does a very good job of removing BNB-related backgrounds as well, for the virtue that BNB muon events share many of the topological features of cosmic muons. Despite the large reduction in background, there are still over 800 BNB-related background events remaining in the $1\gamma1p$ selection and

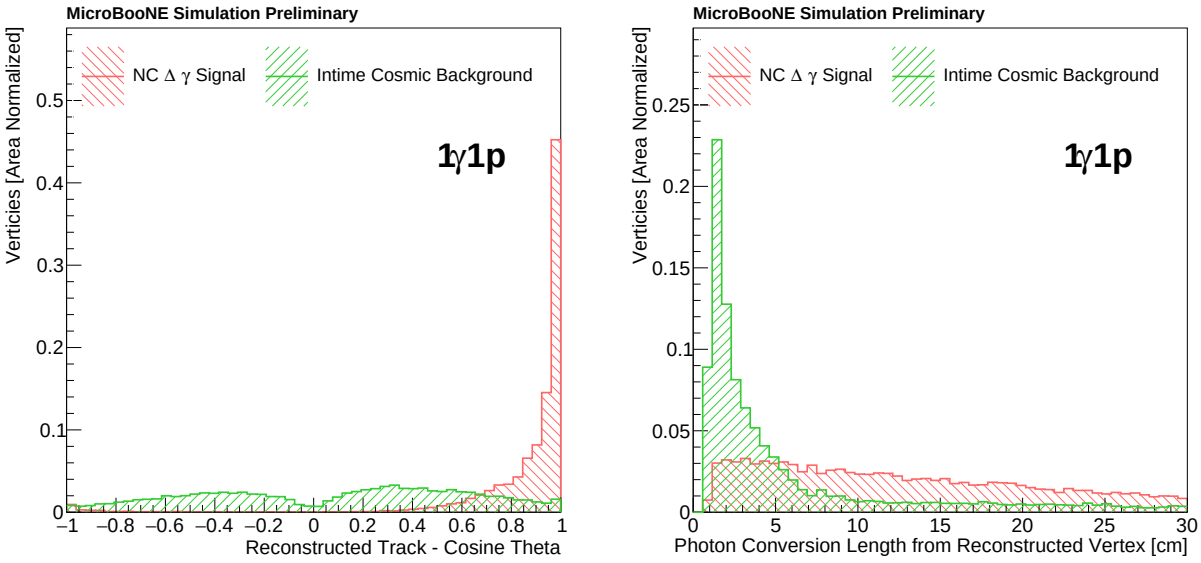

Figure 3: *Left: Comparison of the reconstructed track direction for NC Δ radiative signal (in red) and simulated cosmic background (in-time Corsika Monte Carlo sample, in green), for the* $1\gamma 1p$ *sample used as input to the cosmic-rejection BDT, after passing pre-selection cuts. Right: Similar comparison, but for the separation distance between reconstructed interaction vertex and reconstructed shower start point. Both track direction and vertex-shower separation distance are powerful variables utilized by the cosmic-rejection BDT.*

just under 1000 in the $1\gamma 0p$ selection after cosmic BDT selection. The BDT trained specifically for rejecting the remaining BNB interactions is then applied, reducing total background numbers to $\sim$ 85 and $\sim$ 400 background events for the $1\gamma 1p$ and $1\gamma 0p$ selection, respectively. This corresponds to an impressive cosmic rejection rate of 99.996%, and BNB background rejection rate of 99.94% , for the combined $1\gamma 0p$ and $1\gamma 1p$ selection.

Although backgrounds have been reduced dramatically, the sensitivity to an enhancement to the NC Δ radiative signal at the level necessary to explain the MiniBooNE LEE is still limited. In order to understand and devise plans for further background rejection improvements, the remaining backgrounds are broken down by truth and examined in Sec. 2.6. An example Monte Carlo simulated event display showing a well reconstructed NC Δ radiative decay that passed the event selection is shown in Figure 6.

All main results and efficiencies for all stages of the analysis are shown in Tabs. 1, 2 and 3. Tables 1 and 2 provide a detailed breakdown of how each sample behaves at each stage of the analysis, quoting efficiencies and event rates. Table 3 reformulates this into a total statistical signal significance, as well as recaps the final efficiencies for each sample under study. The total final efficiency for the combined channel is 9.29%.

2.6 Understanding Background Limitations and Further Improvements

This section explores the remaining backgrounds after the current analysis selection, and discussed possible means of improvement by way of further background rejection. Figure 7 provides a breakdown of all background contributions to the $1\gamma 1p$ sample through various selection stages. The figure illustrates the power of the BDTs in removing cosmogenic backgrounds and non-NC BNB-related backgrounds; by the final

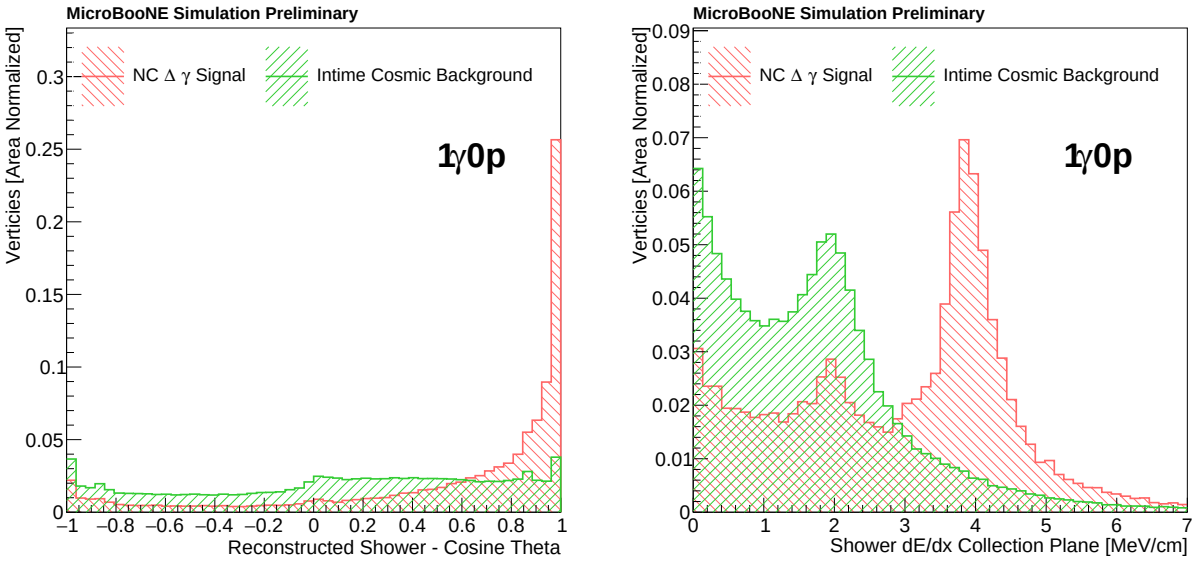

Figure 4: *Left: Comparison of the reconstructed shower direction for NC Δ radiative signal (in red) and simulated cosmic background (in-time Corsika Monte Carlo sample, in green), for the* $1\gamma 0p$ *sample used as input to the cosmic-rejection BDT, after passing pre-selection cuts. Right: Similar comparison, but for the reconstructed shower* dE/dx *averaged over the first 4 cm of the shower. Both shower direction and shower* dE/dx *are powerful variables utilized by the cosmic-rejection BDT.*

selection stage, the most dominant background contribution is that of BNB-related NC π^0 events, accounting for $\approx 85\%$ of the remaining background. NC π^0 events represent a topology that is often indistinguishable (on an event-by-event basis) to that of truly single photon events, as one of the two photons can be missed. As reconstruction algorithms improve, the efficiency with which both photons of a π^0 decay are reconstructed is expected to increase, and this is where current efforts are focused. Statistical methods by which one may estimate the location and energy of a secondary shower are also being explored; however, this approach is still limited by reconstruction efficiencies and resolution especially for low-energy showers. Out of the $\approx 85\%$ NC π^0 background contribution to the final analysis selection (for the $1\gamma 1p$ sample), approximately 20% corresponds to events in which either the second photon exited the active TPC volume or had a true energy of less than 30 MeV. Considering these events as the only potentially irreducible background would suggest that up to a factor of 5 reduction in backgrounds would be possible with improved reconstruction techniques.

To reduce the NC π^0 down as close as possible to the irreducible limit, a second tailored pass of all events that pass the $1\gamma 1p$ selection is being developed. In this second pass, the kinematics of the one reconstructed shower is used to estimate the most probable location and energy of the second missed π^0 daughter photon using the knowledge of the expected π^0 momentum distribution, if indeed it is a true NC π^0 event. Guided by these distributions, a scan for shower-like clusters of hits is performed in each wire-plane of the TPC to look for objects consistent with being the second photon shower from a π^0 decay, even if they were not reconstructed as a shower by Pandora. The possibility of increasing the performance of this is being investigated also, by using a specialized machine learning convolutional neural net (SSnet)[8] to tag all individual hits as being more shower-like or track-like, maximizing the liklihood of being able to find the missed second-showers for NC π^0 decays.

To further constrain the NC π^0 background a dedicated side-band $2\gamma 1p$ topological selection is being per-

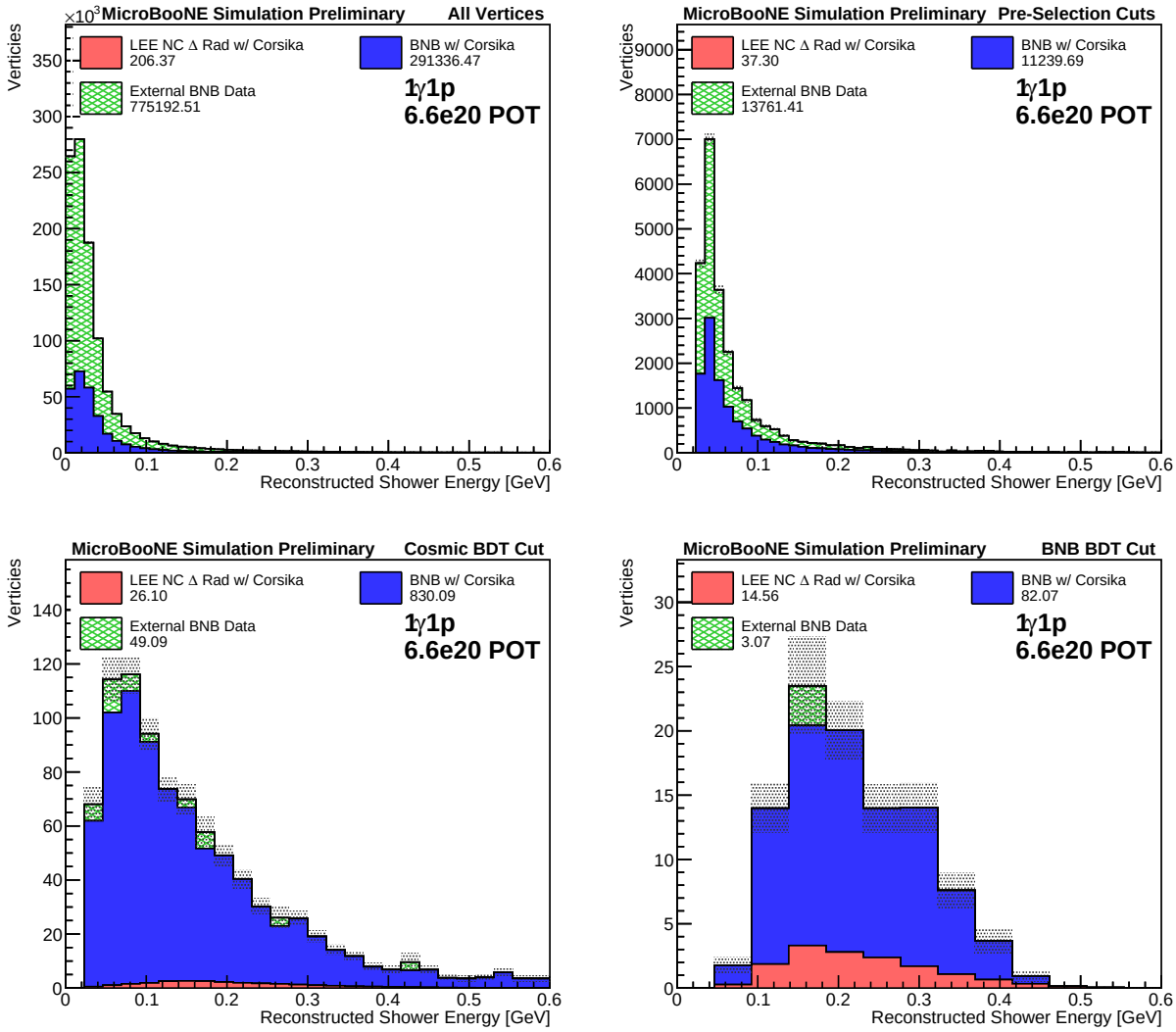

Figure 5: *The evolution of the observable reconstructed shower energy distribution for the* $1\gamma1p$ *selection, through the analysis until we reach the final selection, for a stacked sample of signal and background. All samples are normalized to 6.6E20 POT exposure. The gray shaded regions indicate the Monte Carlo statistical error bars on the total sample. As can be seen, the cosmic BDT cuts the vast majority of the beam spill coincident cosmics out of the sample.*

formed with the goal to select a high purity, high statistics of NC π^0, allowing for a better understanding of the performance and normalization of MicroBooNE Monte Carlo. Once completed, this high purity sample of NC π^0 events would allow us to perform a combined single-photon and NC π^0 fit in order to reduce the systematic uncertainty on the NC π^0 flux and cross-section.

In addition to these analysis specific improvements planned, MicroBooNE has since brought online the cosmic ray tagger (CRT), a veto detector enveloping the MicroBooNE LArTPC, allowing for 85% of total crossing cosmic muons to be tagged by two planes of the CRT. Although the current cosmic rejection BDT performs very well, any improved vetoing of cosmics prior to the BDT stage will allow for a relaxing of the

	LEE NC Δ Radiative w/Cosmics		BNB w/Cosmics		Beam Coincident Cosmic Data	
Stage	Events	Efficiency	Events	Efficiency	Events	Efficiency
Generated	372	100%	654,000	100%	1,990,000	100%
Vertexed	599	161%	710,000	109%	1,900,000	95.6%
Topological	206	55.4%	291,000	44.5%	775,000	39.0%
Total PE > 20	181	48.6% (87.8%)	191,000	29.2% (65.6%)	380,000	19.1% (49.1%)
Fiducial cut	141	37.9% (77.4%)	140,000	21.4% (73.0%)	244,000	12.3% (65.2%)
Track < 100cm	108	29.0% (70.7%)	87,200	13.3% (55.8%)	152,000	7.7% (55.5%)
Reco $E_\gamma > 30$MeV	70.6	19.0% (57.9%)	37400	5.7% (41.9%)	52,500	2.6% (35.3%)
Shower gap > 1cm	57.8	15.5% (78.5%)	25,500	3.9% (72.6%)	37,700	1.9% (73.0%)
Good calo cut	50.2	13.5% (84.4%)	20,600	3.1% (84.4%)	28,600	1.4% (83.0%)
Flipped track cut	40.4	10.8% (71.6%)	12,800	2.0% (66.8%)	16,400	0.8% (65.7%)
Back-to-back cut	37.3	10.0% (83.1%)	11,200	1.7% (80.6%)	13,800	0.7% (78.6%)
All Precuts	37.3	10.0%	11,200	1.72%	13,800	0.69%
Cosmic BDT	26.1	7.01%	830	0.13%	49.1	0.00%
BNB BDT	14.6	3.91%	82.1	0.01%	3.1	0.00%

Table 1: *Summary of number of reconstructed (or selected) vertices for the three main samples used in the $1\gamma 1p$ selection, and corresponding efficiencies, as a function of analysis reconstruction (or selection) stage. The three main samples include the LEE NC Δ radiative with Corsika cosmic Monte Carlo overlays (left 2 columns); BNB backgrounds with Corsika cosmic Monte Carlo overlays (middle 2 columns); and beam-spill coincident cosmic data (right 2 columns). The sequentially applied pre-selection cuts are all listed individually in the middle section of the table. The efficiencies are quoted as number of vertices returned by each stage divided by the number of generated events; each event could have multiple vertices, primarily due to cosmogenic backgrounds. The percentages in brackets refer to the individual efficiency of each pre-selection cut, relative to the topological vertex selection.*

	LEE NC Δ Radiative w/Cosmics		BNB w/Cosmics		Beam Coincident Cosmic Data	
Stage	Events	Efficiency	Events	Efficiency	Events	Efficiency
Generated	372	100%	654,000	100%	1,990,000	100%
Vertexed	599	161%	710,000	109%	1,900,000	95.6%
Topological	147	39.6%	147,000	22.41%	419,000	21.1%
Total PE > 20	132	35.6% (89.9%)	97,600	14.9% (66.6%)	218,000	10.9% (51.9%)
Fiducial cut	113	30.3% (85.1%)	78,900	12.1% (81.6%)	156,000	7.8% (72.8%)
Reco $E_\gamma > 30$MeV	91.1	24.5% (79.5%)	48,900	7.5% (62.6%)	85,600	4.3% (58.7%)
All Precuts	91.1	24.5%	48,900	7.48%	85,600	4.30%
Cosmic BDT	29.6	7.96%	952	0.15%	313.0	0.02%
BNB BDT	20.0	5.38%	320.0	0.05%	82.8	0.00%

Table 2: *Summary of number of reconstructed (or selected) vertices for the three main samples used in the $1\gamma 0p$ selection, and corresponding efficiencies, as a function of analysis reconstruction (or selection) stage. The three main samples include the LEE NC Δ radiative with Corsika cosmic Monte Carlo overlays (left 2 columns); BNB backgrounds with Corsika cosmic Monte Carlo overlays (middle 2 columns); and beam-spill coincident cosmic data (right 2 columns). The sequentially applied pre-selection cuts are all listed individually in the middle section of the table. The efficiencies are quoted as number of vertices returned by each stage divided by the number of generated events; each event could have multiple vertices, primarily due to cosmogenic backgrounds. The percentages in brackets refer to the individual efficiency of each pre-selection cut, relative to the topological vertex selection.*

stringent BDT response cuts leading to increased signal efficiency and sensitivity overall.

	Cosmic BDT cut	BNB BDT cut	Signal Efficiency	Significance ($\frac{s}{\sqrt{b}}$)
$1\gamma 1p$	0.547	0.518	3.91%	1.58 σ
$1\gamma 0p$	0.541	0.527	5.38%	1.00 σ
Combined	-	-	**9.29%**	**1.87** σ

Table 3: *Statistical-only signal significance for each analysis selection sample ($1\gamma 1p$ and $1\gamma 0p$), and for their combination, corresponding to the BDT response cut values as shown in the first two columns, optimized independently for each selection sample, and for 6.6E20 POT.*

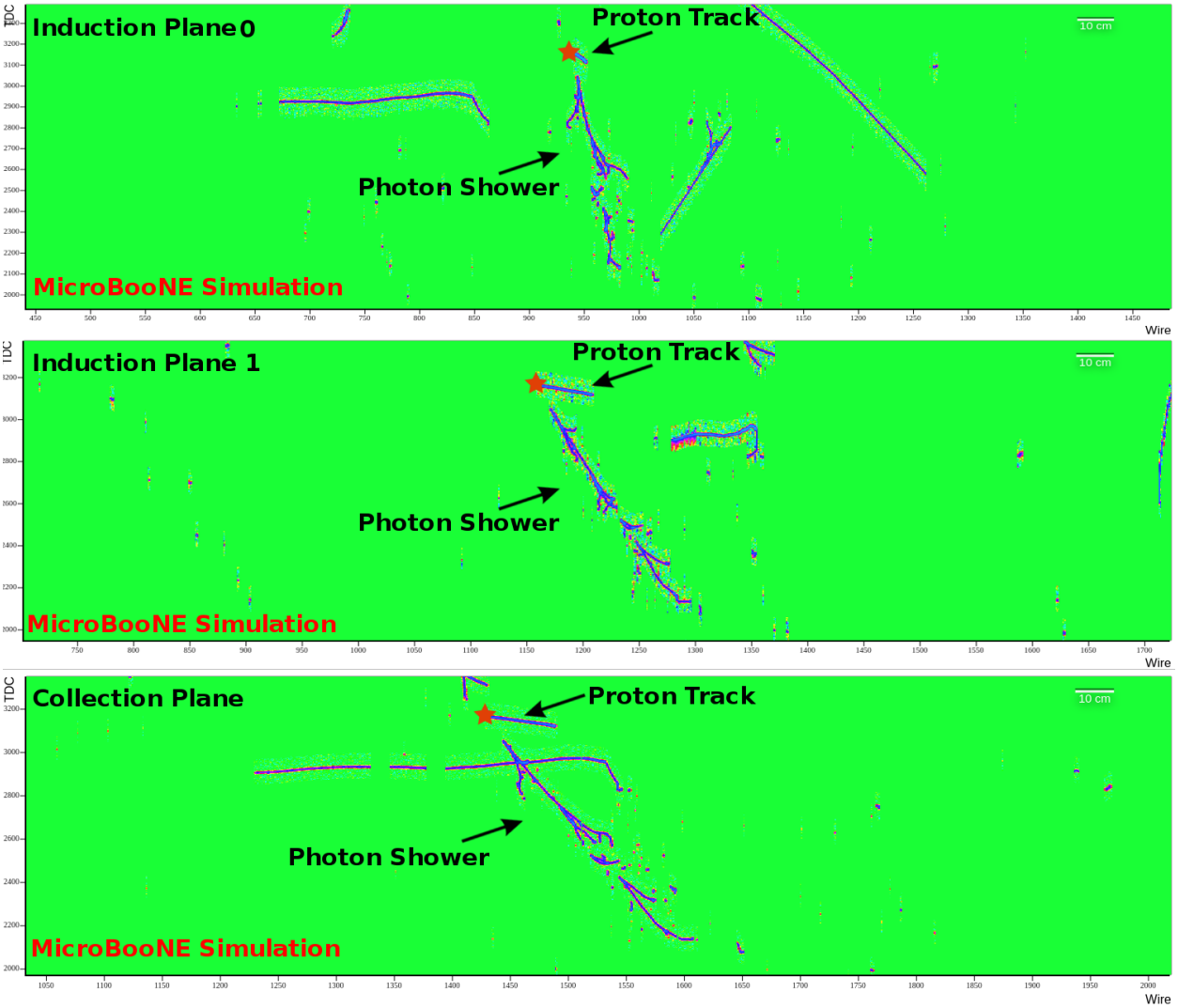

Figure 6: *An example event display of a well-reconstructed NC Δ radiative event (Monte Carlo), showing the ionization recorded in the collection plane (bottom) and two induction planes (top and middle) of the TPC. Reconstructed vertex is shown by the red star. The dE/dx of the shower is $\sim$4 MeV/cm, and there is a clearly identifiable gap between the proton track and where the photon converts into an e^+e^- pair and begins to shower. One can also see several coincidence cosmic muons that occurred in the same beam spill.*

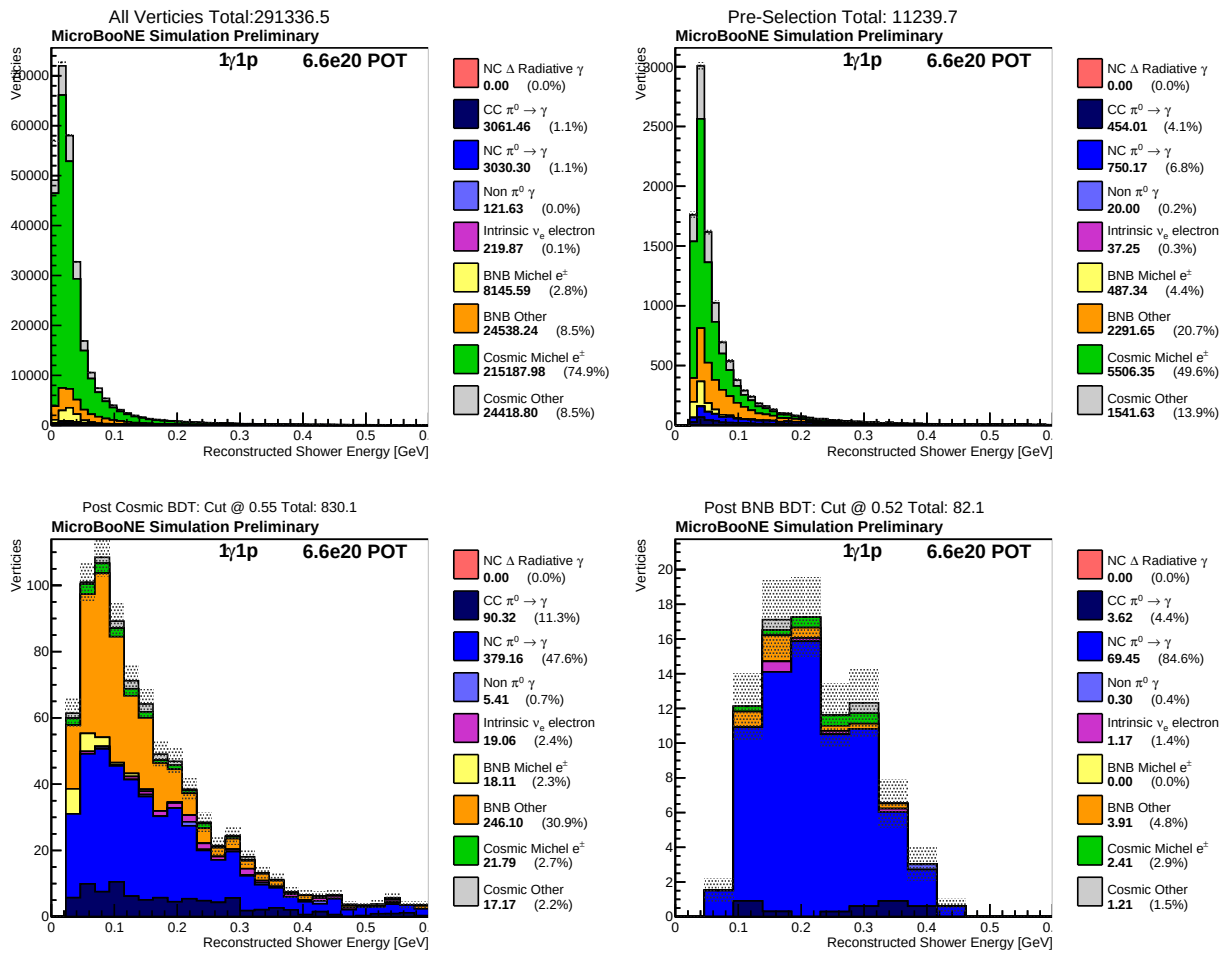

Figure 7: *A breakdown of background contributions based on Monte Carlo as a function of each analysis stage for the $1\gamma1p$ selection. The BNB background contributions are defined according to the final state particle which contributes most dominantly to the reconstructed shower. Monte Carlo statistical uncertainty is shown on the total sum as a gray band. Although the selection is dominated by cosmic-related vertices at the beginning, by the end of the analysis by far the largest remaining background is contributed by NC π^0 events. This is expected, as an NC π^0 in which one photon is lost or mis-reconstructed looks kinematically and calorimetrically similar to an NC Δ radiative event. The NC π^0 background itself consists primarily of events in which the second photon was either not reconstructed or incorrectly merged into another shower object.*

3 Data to Monte Carlo Comparison Validations

Figure 8 provides data and Monte Carlo distribution comparisons after the pre-selection stage of the analysis. This comparison is made using the first 5E19 POT collected by the MicroBooNE detector.[4] The $1\gamma1p$ topological selection distributions are shown in the panels on the left, and the $1\gamma0p$ topological selection distributions are shown in the panels on the right. The top, middle, and bottom rows show these distributions as functions of different reconstructed quantities, namely the reconstructed shower energy (the variable

[4]It is expected that this sample does not contain a statistically significant number of potential signal events.

in which final fits are performed), reconstructed back-projected distance (along the shower direction) from the shower start point to the TPC boundary, and calorimetric shower (track) dE/dx averaged over the first 4 cm of the reconstructed shower (the entire reconstructed track) (bottom right (left)). As of this document certain data quality cuts have not yet been applied which will affect about 10% of the sample.

Spectral agreement is reasonable across all variables shown in this figure as well as all of the remaining variables which are fed into the subsequent BDT training and selection stages. A slight (4.4%) normalization excess of events in the $1\gamma 0p$ sample with respect to the Monte Carlo predictions is seen; this however is well within current flux and systematic uncertainties. As there are several more track based pre-selection cuts applied to the $1\gamma 1p$ selection, the statistics in both data and MC samples that pass reflect this accordingly, with the $1\gamma 0p$ having more than 5x times $1\gamma 1p$ statistics.

There are several additional ongoing studies that are being performed before data-mc comparisons of the BDT responses will be evaluated, including an analysis of the impact of events containing neutrino induced interactions originating outside the fiducial volume that scatter in (so called dirt events), as well a detailed investigation into the systematic uncertainties on the flux, cross-section and detector simulation of MicroBooNE.

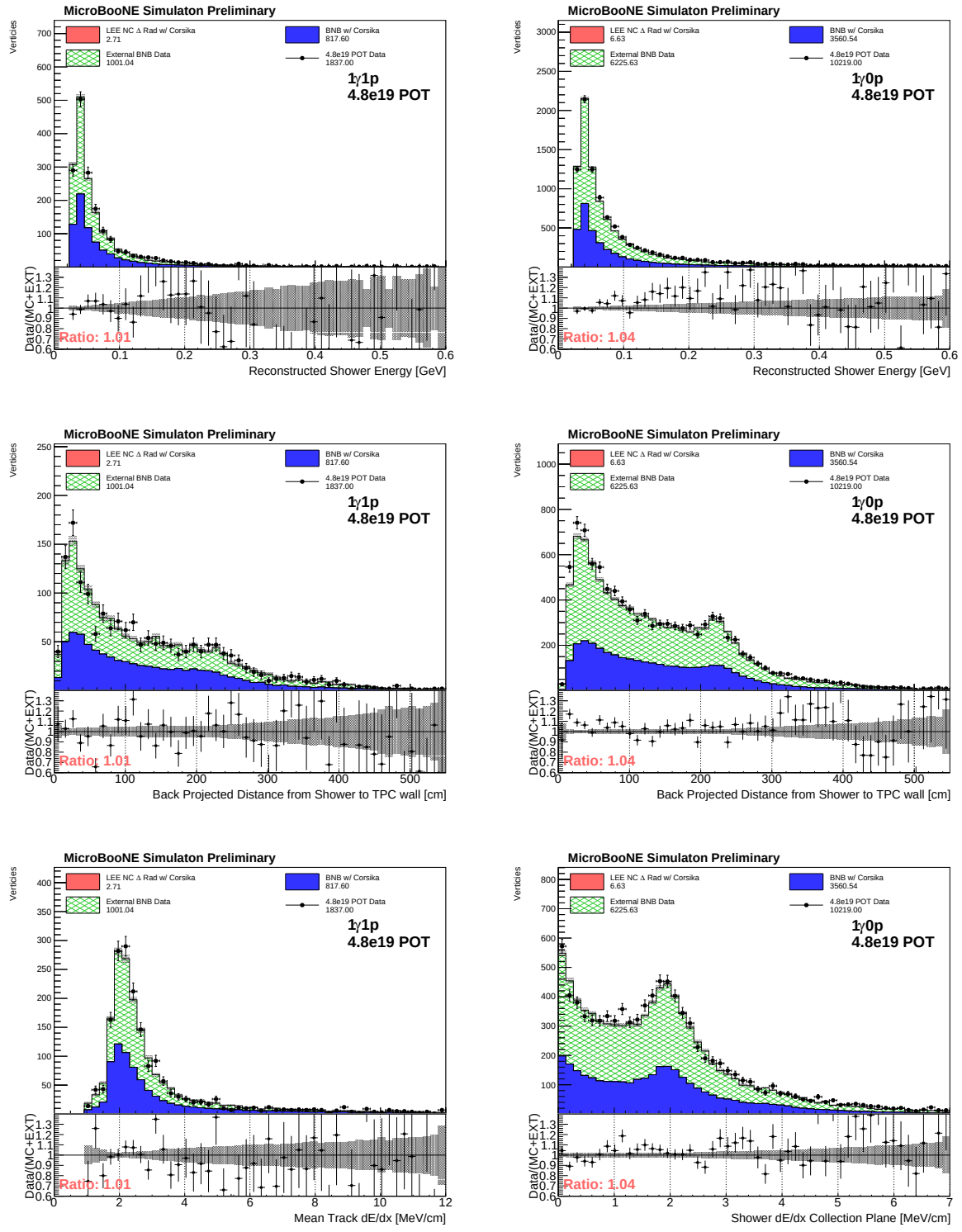

Figure 8: *Data to Monte Carlo comparisons for the* $1\gamma1p$ *(left) and* $1\gamma0p$ *topological selections, for 4.8E19 POT, provided as distributions of several reconstructed variables of interest: reconstructed shower energy (top); reconstructed back-projected distance (along the shower direction) from the shower start point to the TPC boundary (middle); and calorimetric shower* dE/dx *averaged over the first 4 cm of the reconstructed shower (bottom right) and calorimetric track* dE/dx *averaged over the full reconstructed track length (bottom left). The bottom panel of each figure shows the ratio of the observed data to total prediction (stacked Monte Carlo and beam-spill coincidence cosmic data). The gray shaded error band represents Monte Carlo and beam-spill coincidence cosmic data statistical errors, whereas the data statistical error is shown on each point.*

4 Projected Physics Sensitivities

Figure 9 shows the expected MicroBooNE sensitivity to a potential NC Δ radiative cross-section enhancement (left panel) using the full anticipated data set of 6.6E20 POT, constructed using the CLs method [9]. An enhancement of a factor of 4.6 can be excluded at the 99% confidence level (CL), providing a competitively sensitive measurement of (or limit to) the neutrino NC Δ radiative decay cross-section[5]. In the same figure, the NC Δ radiative decay interpretation of the MiniBooNE LEE can be represented as an enhancement of a factor of 3, indicated by the vertical black line on the figure. To investigate what level of sensitivity improvement is possible in terms of additional background rejection that may be achievable through the (ongoing) analysis presented in this note, the sensitivity to the LEE interpretation (factor of 3 enhancement) is cast in terms of additional background rejection factor in Fig. (10). An additional background reduction of a factor of approximately 2.2 would be necessary for >99% CL statistics-only sensitivity.

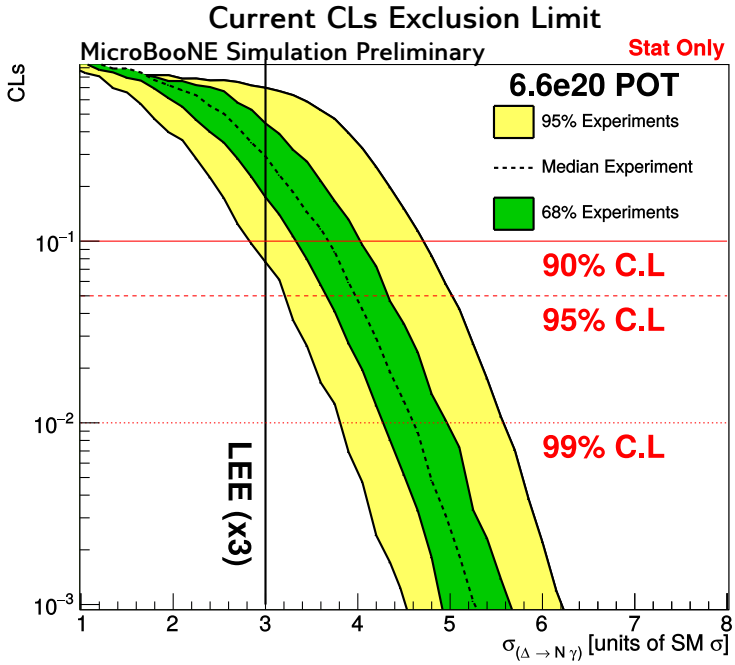

Figure 9: *MicroBooNE sensitivity to the NC $\Delta \to N\gamma$-like cross-section, as well as to the MiniBooNE low energy excess, if interpreted as NC $\Delta \to N\gamma$-like process. The sensitivity is represented by the CLs parameter, and corresponds to the projected statistical-only sensitivity for the full 6.6×10^{20} POT.*

[5]The T2K experiment has publicized bounds [10] which are at least an order of magnitude less sensitive than what is presented in Fig. 9.

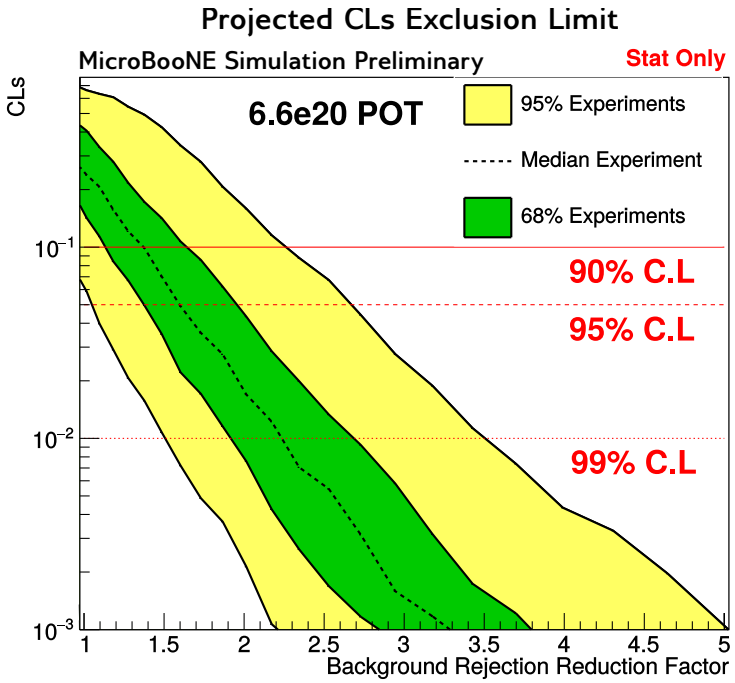

Figure 10: *For a fixed enhancement factor of 3 times the standard model prediction, corresponding to the requirements of the MiniBooNE LEE, this plot shows the effect of further background reduction on the projected MicroBooNE sensitivity to a NC $\Delta \rightarrow N\gamma$-like interpretation of the MiniBooNE LEE.*

5 Summary and Conclusions

The MicroBooNE search for neutrino-induced NC single photon events has been presented, optimized for a NC Δ radiative decay signal prediction. This search can be applied to constrain the standard-model predicted rate of this process, as well as to test an NC Δ radiative decay interpretation of the previously observed MiniBooNE low energy excess. The analysis demonstrates the challenge of low-energy shower reconstruction in LArTPCs and ongoing efforts are targeting improvements in shower reconstruction efficiency in particular at low energy. At this stage, statistical-only sensitivities have been considered in evaluating the analysis sensitivity, and preliminary data to Monte Carlo comparisons using the 4.8e19 POT of available unblinded data have been performed.

The statistical sensitivity achievable to a NC Δ radiative decay interpretation of the MiniBooNE observed LEE is currently expected to be 1.87σ for 6.6E20 POT; it is possible to improve this to the level of $> 99\%$ CL if the current background contributions could be reduced by a factor of 2.2; however, we note this is a conservative estimate as any improvements in background rejection would allow for relaxing of the currently rather aggressive BDT cuts. The current selection applied to the full 6.6E20 POT data set would exclude cross-sections 4.6 times the standard model value at the 99% C.L. for the median experiment, considering statistic uncertainties only. Ongoing efforts are also targeting the further rejection of NC π^0 backgrounds, which are the dominant background contribution. Those can be mitigated through improvements in shower clustering and reconstruction, as well as tailored searches for the second, missed, shower in NC π^0 events that currently pass the analysis selection chain.

References

[1] R. Acciarri et al. Design and Construction of the MicroBooNE Detector. *JINST*, 12(02):P02017, 2017.

[2] A. A. Aguilar-Arevalo et al. Unexplained Excess of Electron-Like Events From a 1-GeV Neutrino Beam. *Phys. Rev. Lett.*, 102:101802, 2009.

[3] JL. Rosner. Low-energy photon production in neutrino neutral-current interactions. *Phys. Rev.*, D91(9):093001, 2015.

[4] C. Andreopoulos et al. The GENIE Neutrino Monte Carlo Generator: Physics and User Manual. 2015.

[5] J. S. Marshall and M. A. Thomson. The Pandora Software Development Kit for Pattern Recognition. *Eur. Phys. J.*, C75(9):439, 2015.

[6] MicroBooNE Collaboration. Microboone low-energy excess signal prediction from unfolding. *MicroBooNE Public Note 1043*.

[7] D. Heck, J. Knapp, J. N. Capdevielle, G. Schatz, and T. Thouw. *CORSIKA: a Monte Carlo code to simulate extensive air showers.* February 1998.

[8] R. Acciarri et al. Convolutional Neural Networks Applied to Neutrino Events in a Liquid Argon Time Projection Chamber. *JINST*, 12(03):P03011, 2017.

[9] A L Read. Presentation of search results: the cl s technique. *Journal of Physics G: Nuclear and Particle Physics*, 28(10):2693, 2002.

[10] E. Hernandez, J. Nieves, M. Valverde, and M. J. Vicente-Vacas. New determination of the N-$\Delta(1232)$ axial form factors from weak pion production and coherent pion production off nuclei at T2K and MiniBooNE energies revisited. *AIP Conf. Proc.*, 1382:153–155, 2011.